Materials International
Open Access Journal (ISSN: 2668-5728)

Article
Volume 4, Issue 1, 2022, 2
https://doi.org/10.33263/Materials41.002

Tuning the Electronic and Magnetic Properties of Fe_3Se_4 Material by Mechanical Strain

Sunita J. Yadav [1,*], Jaykumar Jasani [1], Sandip R. Kumavat [1], Deobrat Singh [2], Dimple V. Shah [1,*], Yogesh Sonvane [2,*], Rajeev Ahuja [2,3]

[1] Material Science Lab, Department of Physics, Sardar.Vallabhbhai. National Institute of Technology, Surat, India
[2] Condensed Matter Theory Group, Materials Theory Division, Department of Physics and Astronomy, Uppsala University, Box 516, 75120 Uppsala, Sweden
[3] Department of Physics, Indian Institute of Technology Ropar, Rupnagar 140001, Punjab, India
* Correspondence: yadavsunitajeetubhai@gmail.com (S.J.Y.);dshah@phy.svnit.ac.in (D.V.S); yas@phy.svnit.ac.in (Y.S.)
Scopus Author ID 37066486600

Received: 16.01.2022; Accepted: 20.02.2022; Published: 9.03.2022

Abstract: Study of strain-dependent magnetic properties of Fe_3Se_4 material through density functional theory. The structural and electronic properties were also studied. From the analysis of its electronic band structures and state density, we have found out that there is a hybridization of Fe-3d and Se-4p states at the Fermi level. So, from our study, we find metallic band structure (electronic states of up and down spin crosses the Fermi level) for this system, and hence it shows metallic behavior, while from the density of states, it was shown that the Fe atoms contribute more than Se atom at the Fermi level and it is mainly due to the Fe-3d states. We have also found out its magnetic moment, which comes out to be 4.29μ_B per unit cell. We have also applied mechanical strain in compressive and tensile strain and studied its effect on the magnetic moment. Variation in the magnetic moment is noticed due to the applied strain. This Fe_3Se_4 material has its application in spintronics and various magnetic storage devices.

Keywords: mechanical strain; density functional theory; magnetic properties; magnetic moment; band structure; state density.

1. Introduction

Since 1950, we have studied iron chalcogenides compounds [1-4]. Fe_3Se_4 and Fe_7Se_8 are the two magnetic compounds in which Fe and Se along the C-axis occupy layers alternate. Curie temperatures of Fe_3Se_4 and Fe_7Se_8 are 314 K and 450 K [1-4]. Here, we have studied about Fe_3Se_4. Fe_3Se_4 and Fe_7Se_8 are hard magnetic materials that recently got attention because of their magnetic and electrical properties. It was observed that this Fe_3Se_4 material has a large coercivity at room temperature [5]. So, These magnetic materials have their applications in permanent magnets and high-density data storage due to their large coercivity [6,7]. As the atomic number of anions increases as we go to Te from O., covalency between the d orbitals of transition-metal and the p orbitals of anion becomes hard; hence we can say that movement of d electrons in transition-metal chalcogenides is more than that in oxides [8]. Hirone and Chiba were the first to study the magnetism of iron selenides. They have found 303 K Curie temperature for this Fe_3Se_4, where Terzieff and Komamk also studied magnetic properties and got the Curie temperature 338 K; we got these differences because of the variation in compositions found in the solid-solution range [9]. In the present paper, we aim to gain a

fundamental understanding of the lattice structure, electronic DOS and band structure, and the magnetic behavior of this ferromagnetic material through density functional theory [10]. We also aim to study the variation of the magnetic moment due to the applied mechanical strain.

2. Materials and Methods

2.1. Methodology

Here, spin-polarized density functional theory is used to calculate through VASP [11-14] software. By taking the Perdew–Burke-Ernzerhof (PBE) as exchange-correlation functional [15-20] in the generalized gradient approximation (GGA) scheme, we have solved the Kohn-Sham equations [21-28]. We have taken the energy cut-off for plane-wave basis set to form electronic wave function as 500 eV. For electronic DOS and band structure calculations, the k-points which we have used is 15×15×15, and for optimization of the structure, we have used 5×5×5 k-points [22]. We have optimized lattice parameters and the positions of atoms for force and pressure below 10^{-3} eV/Å within the space group of 12/m (monoclinic phase).

3. Results and Discussion

3.1. Structural properties.

We have studied strain-dependent magnetic properties of Fe_3Se_4 through the density functional theory approach. We have also obtained the fully optimized crystal structure of Fe_3Se_4 for a single unit cell, as shown in Figure 1(a). Here, we have considered 3 atoms of iron and 4 atoms of selenium. From this optimized crystal structure, the bond length between the atoms bond angle between atoms was known. The optimized angle between any three atoms Fe-Se-Fe is 70.395º, and between Se-Fe-Se is 91.193º, and the bond length between Fe-Se is 2.574 Å and between Fe-Fe is 2.890 Å. The lattice constants for our structure are found to be a=3.45 Å, b=6.07 Å, and c=6.35 Å. we have also optimized the lattice constant as shown in Figure 1(b-d). We have also done energy cut-off optimization and k-points optimization to get the exact values for the same.

3.2. Electronics properties

The electronic properties of Fe_3Se_4 were studied, as shown in Figure 2. Figure 2(a) shows the total density of states and their contribution to the individual atom. From the electronic configuration of Fe and Se, it can be seen that the 3d orbitals of Fe and 4p orbitals of Se are taking part in this density of states. Figure 2(a) clearly shows that the Fe atom will contribute more to the density of states than the Se atom at the Fermi level. We have also calculated the electronic band structure, shown in Figure 2(b). Figure. 2(c),(d) shows the spin-up and spin-down band structure of Fe_3Se_4. The valence and conduction bands overlap at the Fermi level, and we got a zero bandgap. Hence we can say that Fe_3Se_4 shows metallic nature.

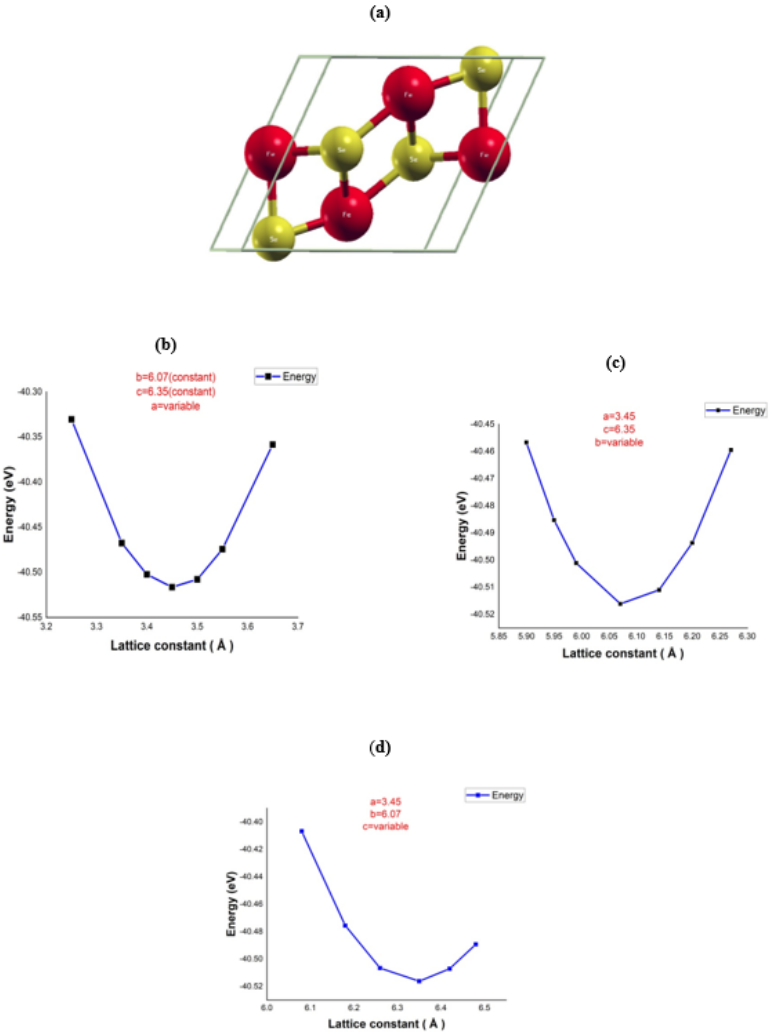

Figure 1. (a) The fully optimized crystal structure of Fe_3Se_4, (b),(c),(d) shows constant lattice optimization of each lattice constant

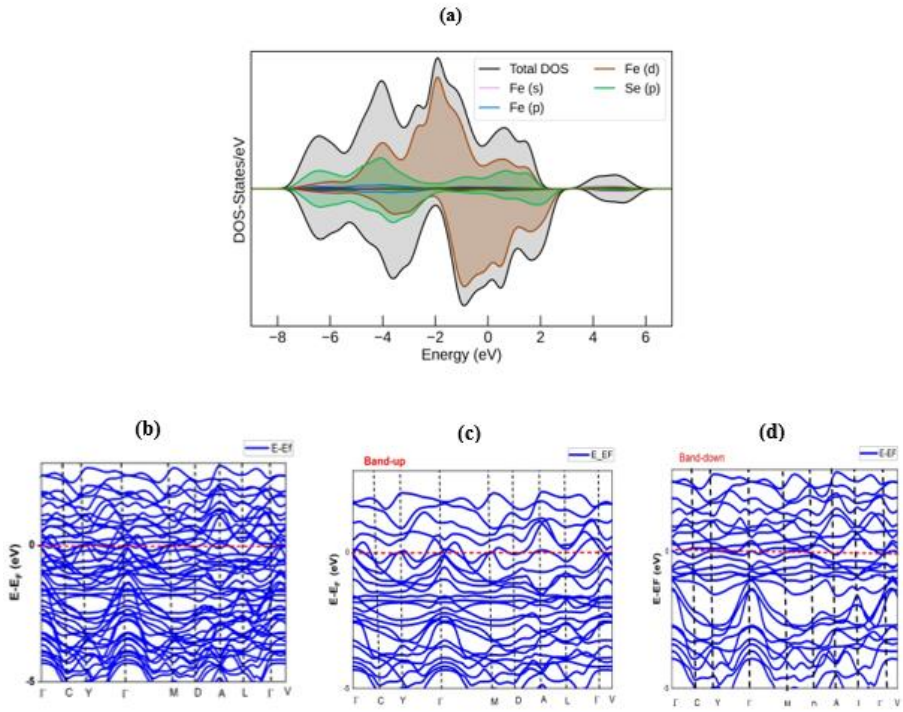

Figure 2. (a) shows the density of states of Fe_3Se_4. (b) electronic band structure of Fe_3Se_4 (c) band-up and (d) band-down also calculated for Fe_3Se_4

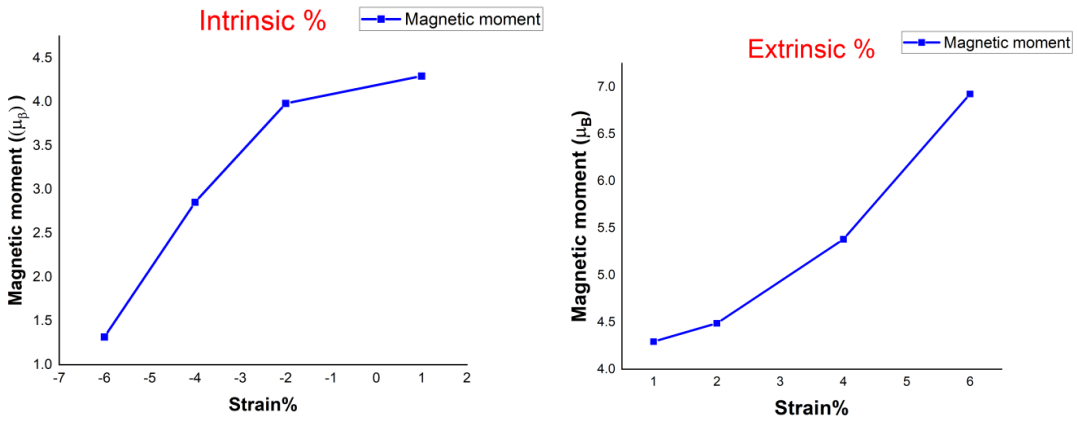

Figure 3. (a) Intrinsic strain of Fe_3Se_4 and (b) Extrinsic strain of Fe_3Se_4.

3.3. Magnetic properties.

The unit cell of Fe_3Se_4 material has 6 atoms of Fe and 8 atoms of Se in the monoclinic phase. Due to the presence of Fe atoms in this structure, we got a magnetic moment of 4.29 μ_B which is good consistent with previous literature. Further, when we applied extrinsic strain, the magnetic moment drastically changed in increasing order, as shown in Figure 3(a). While, when an intrinsic strain is applied, the magnetic moment changes significantly in decreasing order, as shown in Figure 3(b).

4. Conclusions

We have investigated the electronic and magnetic properties of Fe_3Se_4 through the density functional theory approach. It was observed that this material shows metallic behavior whose magnetic moment comes out to be 4.29 μ_B per unit cell. Because of the large permanent magnetic moment, this material is used in spintronics and magnetic storage devices. Due to applied mechanical strain in increasing or decreasing order, the changes in a magnetic moment in increasing and decreasing order are noticed.

Funding

This research received no external funding.

Acknowledgments

I would like to express my special thanks and gratitude to Dr. Deobrat Singh, Dr. Dimple V. Shah, and Dr. Yogesh Sonvane, as well as the MHRD, for their support. Secondly, I would also like to thank Jaykumar Jasani, Sandip R. Kumavat, and all my friends who are helping me a lot in my research. It helped me to increase my knowledge and skills.

Conflicts of Interest

The authors declare no conflict of interest.

References

1. Hirone, T.; Chiba, S. The Magnetic Properties of FeSex with the NiAs Structure. *Journal of the Physical Society of Japan* **1956**, *11*, 666-670, https://doi.org/10.1143/JPSJ.11.666.

2. Okazaki, A.; Hirakawa, K. Structural Study of Iron Selenides FeSex. I Ordered Arrangement of Defects of Fe Atoms. *Journal of the Physical Society of Japan* **1956**, *11*, 930-936, https://doi.org/10.1143/JPSJ.11.930.
3. Hirakawa, K. The Magnetic Properties of Iron Selenide Single Crystals. *Journal of the Physical Society of Japan* **1957**, *12*, 929-938, https://doi.org/10.1143/JPSJ.12.929.
4. Kamimura, T.; Kamigaki, K.; Hirone, T.; Sato, K. On the Magnetocrystalline Anisotropy of Iron Selenide Fe7Se8. *Journal of the Physical Society of Japan* **1967**, *22*, 1235-1240, https://doi.org/10.1143/JPSJ.22.1235.
5. Zhang, H.; Long, G.; Li, D.; Sabirianov, R.; Zeng, H. Fe3Se4 Nanostructures with Giant Coercivity Synthesized by Solution Chemistry. *Chemistry of Materials* **2011**, *23*, 3769-3774, 2011https://doi.org/10.1021/cm201610k.
6. Zhang, H.-W.; Liu, Y.; Sun, S.-H. Synthesis and assembly of magnetic nanoparticles for information and energy storage applications. *Frontiers of Physics in China* **2010**, *5*, 347-356, https://doi.org/10.1007/s11467-010-0104-9.
7. Sun, S.; Murray, C.B.; Weller, D.; Folks, L.; Moser, A. Monodisperse FePt nanoparticles and ferromagnetic FePt nanocrystal superlattices. *Science* **2000**, *287*, 1989-1992, https://doi.org/10.1126/science.287.5460.1989.
8. Shimada, K.; Mizokawa, T.; Mamiya, K.; Saitoh, T.; Fujimori, A.; Ono, K.; Kakizaki, A.; Ishii, T.; Shirai, M.; Kamimura, T. Spin-integrated and spin-resolved photoemission study of Fe chalcogenides. *Physical Review B* **1998**, *57*, 8845-8853, https://doi.org/10.1103/PhysRevB.57.8845.
9. Li, S.; Jin, S.F.; Ji, J.; Guo, Z.N.; Yuan, W.X. Investigation on solid solubility and magnetism of the non-stoichiometric compound Fe3Se4. *Powder Diffraction* **2013**, *28*, S32-S36, https://doi.org/10.1017/S0885715612001030.
10. Singh, D.; Gupta, S.K.; He, H.; Sonvane, Y. First-principles study of the electronic, magnetic and optical properties of Fe3Se4 in its monoclinic phase. *Journal of Magnetism and Magnetic Materials* **2020**, *498*, https://doi.org/10.1016/j.jmmm.2019.166157.
11. Kresse, G.; Furthmüller, J. Efficient iterative schemes for ab initio total-energy calculations using a plane-wave basis set. *Physical Review B* **1996**, *54*, 11169-11186, https://doi.org/10.1103/physrevb.54.11169.
12. Kumavat, S.R.; Sonvane, Y.; Gupta, S.K. Structural, optical, transport, and solar cell properties of 2D halide perovskite MAZX3 (Z = Pb, Sn, and X = Cl, Br, I). *Journal of Applied Physics* **2020**, *128*, https://doi.org/10.1063/5.0016331.
13. Kumavat, S.; Singh, D.; Sonvane, Y.; Gupta, S.K. Ab-initio study of strain engineering optical properties of RbPbI3. *AIP Conference Proceedings* **2019**, *2115*, https://doi.org/10.1063/1.5112993.
14. Kumavat, S.; Sonvane, Y.; Gupta, S.K. Lattice strain dependent optical properties of BaSnO3: First principle study. *AIP Conference Proceedings* **2020**, *2265*, https://doi.org/10.1063/5.0017369.
15. Perdew, J.P.; Burke, K.; Ernzerhof, M. Generalized Gradient Approximation Made Simple. *Physical Review Letters* **1996**, *77*, 3865-3868, https://doi.org/10.1103/physrevlett.77.3865.
16. Mishra, P.; Singh, D.; Sonvane, Y.; Ahuja, R. Metal-functionalized 2D boron sulfide monolayer material enhancing hydrogen storage capacities. *Journal of Applied Physics* **2020**, *127*, https://doi.org/10.1063/5.0008980.
17. Patel, A.; Singh, D.; Sonvane, Y.; Thakor, P.B.; Ahuja, R. High Thermoelectric Performance in Two-Dimensional Janus Monolayer Material WS-X (X = Se and Te). *ACS applied materials & interfaces* **2020**, *12*, 46212-46219, https://doi.org/10.1021/acsami.0c13960.
18. Somaiya, R.N.; Singh, D.; Sonvane, Y.; Gupta, S.K.; Ahuja, R. Potential SiX (X = N, P, As, Sb, Bi) homo-bilayers for visible-light photocatalyst applications. *Catalysis Science & Technology* **2021**, *11*, 4996-5013, https://doi.org/10.1039/D1CY00304F.
19. Yadav, P.; Dev Bhuyan, P.; Rout, S.K.; Sonvane, Y.; Gupta, S.K.; Sinha, E. Correlation between experimental and theoretical study of scheelite and wolframite-type tungstates. *Materials Today Communications* **2020**, *25*, https://doi.org/10.1016/j.mtcomm.2020.101417.
20. Mishra, P.; Singh, D.; Sonvane, Y.; Ahuja, R. Excitonic effects in the optoelectronic properties of graphene-like BC monolayer. *Optical Materials* **2020**, *110*, https://doi.org/10.1016/j.optmat.2020.110476.
21. Burke, K.; Perdew, J.P.; Wang, Y. Derivation of a Generalized Gradient Approximation: The PW91 Density Functional. In: *Electronic Density Functional Theory: Recent Progress and New Directions*. Dobson, J.F.; Vignale, G.; Das, M.P. Eds.; Springer US: Boston, MA, **1998**; pp. 81-111, https://doi.org/10.1007/978-1-4899-0316-7_7.
22. Somaiya, R.N.; Sonvane, Y.; Gupta, S.K. Van der waals SiSe2 homo-bilayers for optoelectronics applications. *Superlattices and Microstructures* **2021**, *152*, https://doi.org/10.1016/j.spmi.2021.106858.
23. Patel, V.R.; Patel, A.; Sonvane, Y.; Thakor, P.B. Optoelectronic properties of 2D heterojunction ZrO2– MoS2 material using first-principles calculations. *Solid State Communications* **2021**, *334-335*, https://doi.org/10.1016/j.ssc.2021.114358.
24. Somaiya, R.N.; Sonvane, Y.; Gupta, S.K. Adsorption of toxic gas molecules on the pre-oxidized Cu2Si nanosheet – A DFT study. *Computational Materials Science* **2020**, *173*, https://doi.org/10.1016/j.commatsci.2019.109414.

25. Mahida, H.R.; Singh, D.; Sonvane, Y.; Gupta, S.K.; Thakor, P.B.; Ahuja, R. Hydrogenation and oxidation enhances the thermoelectric performance of Si2BN monolayer. *New Journal of Chemistry* **2021**, *45*, 3892-3900, https://doi.org/10.1039/D0NJ06000C.
26. Singh, S.; Sonvane, Y.; Nekrasov, K.A.; Boyarchenkov, A.S.; Kupryazhkin, A.Y.; Gajjar, P.N.; Gupta, S.K. Ab-initio investigation of crystal structure and pressure induced phase transition in ThO2 and PuO2. *Materials Today Communications* **2021**, *28*, https://doi.org/10.1016/j.mtcomm.2021.102579.
27. Kansara, S.; Sonvane, Y.; Gupta, S.K. Modulation of vertical strain and electric field on C3As/arsenene heterostructure. *Applied Nanoscience* **2020**, *10*, 107-116, https://doi.org/10.1007/s13204-019-01034-0.
28. Singh, D.; Gupta, S.K.; Hussain, T.; Sonvane, Y.; Gajjar, P.N.; Ahuja, R. Antimonene Allotropes α- and β-Phases as Promising Anchoring Materials for Lithium–Sulfur Batteries. *Energy & Fuels* **2021**, *35*, 9001-9009, https://doi.org/10.1021/acs.energyfuels.1c00607.